12th International Congress on the Deterioration and Conservation of Stone
Columbia University, New York, 2012

ROLE OF SWELLING CLAY MINERALS IN THE SPALLING DECAY MECHANISM OF THE "PIERRE DU MIDI" LIMESTONE (SOUTH-EAST OF FRANCE)

Jérémie Berthonneau[1,2,3], Olivier Grauby[2], Philippe Bromblet[3], Jean-Marc Vallet[3], David Dessandier[1] and Alain Baronnet[2]

[1] *BRGM, 3 Av. Claude-Guillemin B.P. 36009, 45060 Orléans Cedex 2, France.*
[2] *CINaM-CNRS & Aix-Marseille Université, France.*
[3]*CICRP Belle-de-Mai, 21 rue Guibal, 13003 Marseille, France.*

Abstract

Widely used into Provençal building heritage, the "Pierre du Midi" shows a heterogeneous durability *in situ*. While some historical buildings made up with this Burdigalian (Miocene) limestone do not display any superficial modification, others show specific stone deterioration pattern called spalling after comparable time of exposure. With variable extent, this decay pattern sometimes includes the loss of rock fragments. The affected stones are located on the upper façade parts, subjected to the stronger climatic variations, but free from salt weathering, mechanical charges, biologic colonization or atmospheric pollution. In order to understand the decay process triggered by the climatic variations, the present study aims to define the internal properties involved in the macroscopical mechanical behavior leading to spalling. Eight stone types, representative of the material heterogeneity, were collected from both active and given up quarries spread inside four geological sub-basins located in the South-East of France. The extraction sites have first been replaced inside the sedimentological profile of Miocene deposits. Then, comparison of common hydro-mechanical characteristics (including mineralogy, water transfer properties, hygric and hydric dilatation) with the decay extent has shown the occurrence of mixed-layer minerals containing smectitic layers in the most subjected samples to spalling. As these smectitic layers are known to undergo intracristalline swelling upon water content variation, a specific attention has been given on their quantification by combining mineralogical and chemical methods : oriented X-ray diffractogram fitting procedure, and TEM-EDS analysis of the infra 4µm fraction. The relationships between swelling clay minerals proportion, their location and the dilatometric behavior measured are finally discussed into the frame of this study.

Keywords: spalling, clay minerals, hydric and hygric expansion, intracristalline swelling.

1. Introduction

A large part of the building heritage dated between the 1st century and the XVIIth century in the PACA region (South East of France) have been erected using a bioclastic limestone commonly named "Pierre du Midi". On the basis of their extraction site, different limestone types have been distinguished. And, once exposed to environmental conditions a heterogeneous durability can be observed. On one hand, among others deterioration patterns, spalling (Vergès-Belmin et al. 2008) is observed on façades of historical buildings Figure 1. After a field campaign, it has been pointed out that the

affected stones are located on the upper façade parts, subjected to the stronger climatic variations, but free from soluble salts, mechanical charges, biologic colonization or atmospheric pollution. Moreover, it sometimes leads to the loss of rock fragments, which justify the regular replacement of a large volume of stones. On the other hand, some limestone types of "Pierre du Midi" are not affected by spalling after comparable times of exposure. Thus internal properties of the affected stones types may play a role in the deterioration process.

Figure 1. Spalling of dimensional stones on the southern façade of Saint Maurice Church (14th century) buildup with Yellow and Grey Caromb stones in Caromb, Vaucluse, France.

Spalling decay has been increasingly studied on sandstones in Europe (Colas et al. 2012; Franzini et al. 2007) and in the world (Jimenez-Gonzalez et al. 2008) in recent years. Authors agree to explain the decay pattern as the result of mechanical stresses at the interface between the wetted exposed surface and the dry inner part during wetting (Sebastian et al. 2008). These stresses are assumed to be driven by the dimensional variations of stones upon water content variation (either in liquid or vapor state). As the physical process involved tends to be understood, the triggering factors of dimensional variations are still controversial. Both the transit of water in micropores and the presence of clay minerals are frequently appealed to explain these dimensional variations (Benavente et al. 2008). But, little has been made on the definition of the nature, the quantity and the location of the clay minerals involved. The present study thus aims to improve our knowledge on the spalling process of "Pierre du Midi" and to investigate the role of swelling clay minerals. Petrophysical characterization including hydric and hygric dilation behavior and clay minerals definition and quantification are presented.

2. Materials

Among the historical buildings from the medieval period into the PACA region six monuments displaying spalling of dimensional stones on their external façades have been studied. Consequently, the "Pierre du Midi" limestones types whose use is

recognized in these monuments were collected in quarries. One of them presenting a variable spalling degree depending on facies, the yellow and the grey Caromb stone types (CARO-J and CARO-G, respectively) were sampled in order to understand this variability. As a matter of comparison, two types of limestones assumed to be free from spalling decay were selected as references. One from a given up quarry (STGA) and the other from an active quarry that provides restoration workshops (ESTA). The studied limestones types and the corresponding historical buildings are presented in Table 1 and ranked according to the extension of spalling decay observed on monuments.

STONE TYPE	SAMPLE	SPALLING DECAY	HISTORICAL MONUMENT STUDIED (city, period of construction)
BARBENTANE Sandstone	BARB	++	Anglica Tower (Barbentane, XIVe)
BIBEMUS Stone	BIBE	++	Saint Sauveur Cathedral (Aix-en-Provence, XII-XVIe)
CAROMB Stone	CARO-G / CARO-J	++ / +	Saint Maurice Church (Caromb, XIVe)
CRILLON Stone	CRIL	+	Saint Romain Church (Crillon, XIVe)
ESTAILLADES Stone	ESTA	-	Notre-Dame-d'Alidon Church (Oppèdes-le-Vieux, XIIIe)
SAINT GABRIEL Stone	STGA	-	Saint-Gabriel Tower (Tarascon, XIIe)
SAINT SYMPHORIEN Stone	STSY	+	High Church of Bonnieux (Bonnieux, XIIe)
VILLENEUVE Stone	VILL	++	Palais des Papes (Avignon, XIVe)

Table 1. List of studied limestones types, samples collected and historical monuments highlighting their behavior through climatic exposure. The degree of spalling decay is also mentioned (-: no superficial modification, +: noticeable spalling, ++: extended spalling and loss of stone fragments).

The extraction quarries of these eight limestone types of the "Pierre du Midi" are located in sedimentological deposits also called "Molasse". During the Miocene period (23-5 Ma) repeated stratigraphic sequences were deposited after cyclic transgression regression alternations. The extracted ones are composed of transgressive cortege of tidal rhythmist dated at the Burdigalian stage (20-16 Ma) and at the Tortonian stage (12 –7 Ma). Petrographic description of the different stones types point out the major composition of bioclasts (Bryozoans, Red Algae, Forams, etc.) surrounded by calcitic matrix and a variable detrital fraction (Quartz, Feldspar, Micas). The intergranular phase appears sometimes as a cement material (STGA) or as a detritic matrix (BARB, CARO-G, VILL). Finally, greenish glauconitic fillings of Bryozoans are observed in all samples except ESTA.

3. Methods

3.1 Mineralogical characterization

The mineralogical composition of the different limestones has been defined on bulk and acetic acid (0.2 N) insoluble fraction with X-ray diffraction. Analyses were performed on disoriented powder using a Brucker D8-Focus diffractometer equipped with a X-ray source tube using Co Kα radiation (λ = 1.7902 Å) at 35 kV and 40 mA. Diffracted intensities were collected by a linear Lynx'Eye detector at 0.01°2θ step intervals from 2 to 80°2θ, using a 1 s counting time per step. In addition, the total fraction of calcium carbonate ($CaCO_3$) has been quantified by "Calcimétrie Bernard" according to the NF X 31-105 standard on < 100 µm powder.

3.2 Petrophysical properties

Petrophysical properties (open porosity, sorptivity, evaporation rate, and ultrasonic velocity) of each stone type were measured on 6 cores (80 mm height and 40 mm diameter) except for VILL whose volume does not allow drilling. Tests were conducted according to the appropriate French standards. The pore network distribution was also examined with mercury intrusion porosimetry (MIP) on ≈ 1 cm^3 samples of each stone type with a Micrormetrics AutoPore IV porosimeter. The MBA test was performed according to the NF EN 933-9 (1999) French standard, with end point determination using the spot test method on dried powders (< 100 µm) of each sample. Tests were considered ended when a light blue colored halo persisted more than 5 min around the dark blue spot. This meaning that free methylene blue was present in solution and thus that all hygroscopic surfaces were covered.

3.3 Definition and quantification of clay minerals

3.3.1 Separation of the clay fraction

The clay fraction of each sample has been defined as < 4 µm instead of < 2 µm normally used as it is reported to better reflect the detrital and authigenic phyllosilicate proportions in bulk samples (Franzini et al. 2007). It was extracted from the acid insoluble fraction by gravitation using Stoke's law. The mass percent of the < 4 µm fractions was determined after eight repeated gravimetric separations and considered to be representative of the total clay fractions even if accessory minerals have been identified. After conscientious deflocculation with hexametaphosphate, the fractions were Ca saturated by repeated cycles of mixing $CaCl_2$ solution (110.9 $g.l^{-1}$) and washing with distilled water.

3.3.2 Crystallo-chemical analysis (TEM-EDS)

After dispersion of the Ca-saturated bulk <4 µm fraction of each sample in distilled water, the suspensions were dropped on copper plates. TEM-EDS analysis on one hundred particles per sample were conducted using a JEOL JEM 2011 TEM fitted with a X-Flash Silicon Drift Detector 5030 (Bruker). Acquisition conditions were set as: x 50 000 magnification, spot size 4^{-2}, tilt 20°, 60 kcps, and a corrected counting time of 30 s. The main elements (O, Na, Mg, Al, Si, K, Ca, Fe) were quantified applying the Cliff-Lorrimer method from spectrums of energy dispersive X-rays after background subtraction (Bremsstrahlung calculation), Gaussian deconvolution, and K-factors correction. Results were processed in order to define structural formulas of each particle with appropriate software and plotted into ternary diagrams M^{+}-4Si-R^{2+} Figure 2. Note that total Fe measured was expressed as Fe_2O_3.

3.3.3 Profile modeling of 00l reflections (XRD)

Oriented aggregates preparations were obtained by pipetting slurries of the Ca-saturated suspension on glass slides. The oriented slides were allowed to dry at room temperature for Air-Dried preparation (AD) and exposed to ethylene glycol (EG) vapor for at least 24 hours. Diffracted intensities were collected on the same Diffractometer than above at 0.014 °2θ step intervals from 2.5 to 60 °2θ, using a 4 s counting time per step. The algorithms developed by Sakharov and Drits (Drits and Tchoubar 1991) were

used to fit the experimental XRD profiles over the 4.5 – 60 °2θ CoKα range using a trial-and-error approach. The fitting strategy consists on obtaining, for a given sample, one structural model that can fit all the diffraction features observed for both the AD and EG experimental patterns. In addition, one essential requirement for assessing the

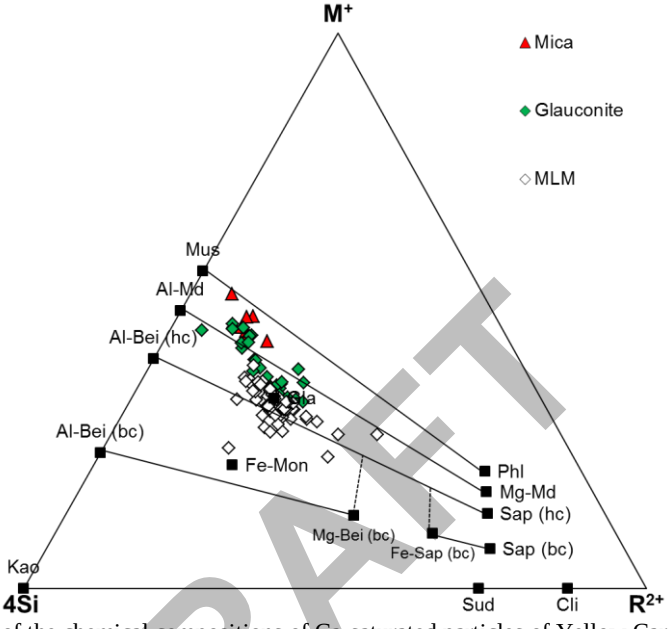

Figure 2. Plot of the chemical compositions of Ca-saturated particles of Yellow Caromb stone type (CARO-J) in the M^+ - 4Si – R^{2+} ternary diagram (adapted from Meunier 2002).

validity of the obtained structure model is that the relative weight contributions of the discrete and mixed-layer clays in a given sample are similar whatever the treatment applied (AD or EG). For each mixed-layer structure, the number, nature, proportion, and layer stacking sequences of the different layer types were considered as adjustable parameters. Each layer type (discrete or mixed-layer) was defined with a unique chemical composition, deduced from the chemical formulas given by the TEM-EDS results, a unique layer thickness, and a unique set of atomic coordinates for all contributions. Results give the relative proportions of the layer types that contribute to the calculated patterns Figure 3, and the relative proportions of specific layers into mixed layer minerals.

3.4 Hydric and hygric dilatation

Maximum dilation coefficient were measured in both hydric and hygric conditions. The direction perpendicular to the bedding plane was used since this direction shows the highest values. Hydric dilation has been calculated from continuous measure of length with a caliper (accuracy of 10 µm) after water imbibition in the same conditions than sorptivity test. Hygric dilatation of samples was defined on one core per sample with RH varying from 30% to 70% and a fixed temperature of 23°C. Displacements were

measured by LVDT sensor (resolution of 0.2 µm) through time using a Solartron® software.

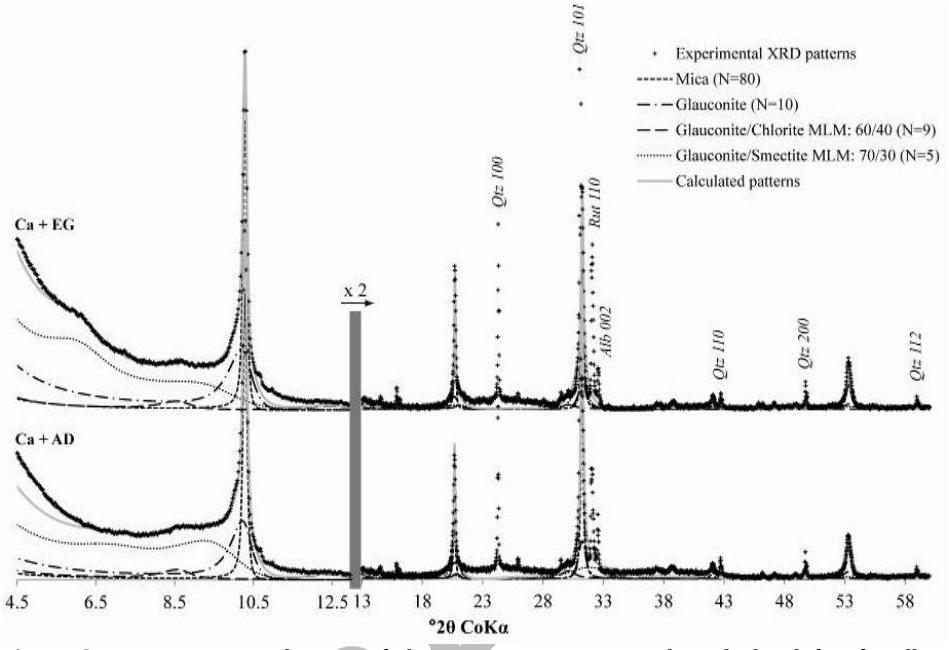

Figure 3. Respective contributions of the various structures to the calculated fit of Yellow Caromb Stone (CARO-J). Accessory minerals are also noted on the diffraction patterns.

4. Results

4.1 Mineralogical composition and physical properties.

Bulk samples compositions vary from pure limestone (ESTA) with more than 99% of $CaCO_3$ to quartzo-limestone with acid insoluble fraction representing from 3.5 to 22.0% of the total mass. Acid insoluble fractions are composed by albite, siderite, hematite and phyllosilicates (mica-like minerals) in various proportions. Table 2 gives the results of porous media and water transfer properties showing the variability of the porous network of "Pierre du Midi" limestone types. First of all, it can be seen that the sample having the higher Hirschwald coefficient (ESTA) is spalling resistant. As a high coefficient is known as a promoting parameter for stone decay (Dessandier et al. 2002) this tends to demonstrate that any common durability factors cannot explain spalling decay.

SAMPLE	ρ_a	N_t	S_{48}	N_{Hg}	r_M	PA_{Hg}	A	$F\ (10^{-3})$	V_d
	$g.cm^{-3}$	%		%	µm	$m^2.g^{-1}$	$kg.m^{-2}.h^{-1/2}$	$kg.m^{-2}.h^{-1}$	$m.s^{-1}$
BARB	2.02	25.5	0.72	25.08	1.46	1.83	127.38	50.25	2550.9
BIBE	-	-	-	17.23	11.22	0.34	-	-	3789.5
CARO-G	-	-	-	18.59	0.05	9.52	-	-	3531.3
CARO-J	2.18	19.8	0.64	23.12	2.29	2.35	102.90	50.32	3671.8
CRIL	2.08	23.3	0.62	21.46	41.73	1.43	206.98	43.55	3442.0
ESTA	1.85	31.7	0.79	-	-	-	994.28	57.14	2534.1
STGA	2.33	13.9	0.62	9.22	1.48	0.48	80.56	29.95	3273.5
STSY	2.06	24.0	0.73	24.28	2.39	1.18	281.53	53.58	3055.9
VILL	-	-	-	30.60	3.90	1.18	-	-	-

Table 2. Main petrophysical properties of samples.

However, the samples the most subjected to spalling (BARB, CARO-G, VILL) display the lower median radius (r_M), and the higher pore area (PA). Finally, sorptivity and ultrasound velocity differ greatly from sample to sample but evaporation rate tends to be homogeneous.

4.2 Clay minerals content

Clay minerals contents defined by gravimetric method ranged from 0.37 % (STGA) to 9.24 % (CARO-G) and are reported in Table 3. TEM-EDS analysis allowed defining the structural formulas of the different clay minerals distinguished chemically. These structural formulas were used in the XRD fitting procedure and helped to distinguish the different nature of clay minerals present in the samples. The overall quantitative data from the fitting procedure are summarized in Table 3.

SAMPLE	BARB	BIBE	CARO-G	CARO-J	CRIL	STGA	STSY	VILL
< 4 µm (*% of total mass*)	0.94	2.23	9.24	3.51	1.08	0.37	0.67	7.85
Glauconite/Smectite MLM	68	5	53	27	39	47	64	31
% of glauconite layers	*55*	*65*	*60*	*70*	*56*	*45*	*45*	*59*
% of smectite layers	*45*	*35*	*40*	*30*	*44*	*55*	*55*	*41*
Mica	15	11	14	41	29	33	14	34
Glauconite	10	12	24	25	23	19	11	27
Chlorite	6	-	10	-	1	1	-	-
Kaolinite	1	-	-	-	-	1	1	1
Glauconite/Chlorite MLM	2	-	-	7	9	-	11	8
% of glauconite layers	*55*	-	-	*60*	*55*	-	*50*	*55*
% of chlorite layers	*45*	-	-	*40*	*45*	-	*50*	*45*
Kaolinite/Glauconite MLM	-	14	-	-	-	-	-	-
% of kaolinite layers	-	*95*	-	-	-	-	-	-
% of glauconite layers	-	*5*	-	-	-	-	-	-
Kaolinite/Smectite MLM	-	61	-	-	-	-	-	-
% of kaolinite layers	-	*79*	-	-	-	-	-	-
% of smectite layers	-	*21*	-	-	-	-	-	-
Smectitic layers (*% of < 4µm*)	31	15	21	8	17	26	35	13
Smectitic layers (*% of sample*)	0.29	0.33	1.94	0.28	0.18	0.10	0.23	1.02

Table 3. Relative mass contributions of the < 4 µm fractions to the bulk samples and the proportions (in percent) of the different clay phases to the diffracted intensity from the simulation of experimental XRD patterns for the AD and EG states (MLM : Mixed Layer Minerals).

Data indicate that the clay mineral fractions mainly consist of Glauconite/Smectite mixed layer minerals with varying proportion of smectitic layers except for one sample

(BIBE). This mixed layer structure, together with the glauconite, being assumed to compose the glauconitic fillings of Bryozoans observed in photonic microscopy. Mica (chemically define as Muscovite), chlorite (sudoïte), glauconite/chlorite and kaolinite are present in most of the sample as minor constituents. Mixed layer minerals of kaolinite/glauconite, and kaolinite/smectite are present in BIBE which deposits period, and thus conditions, differ from others. After computation of the percentage of smectitic layers with the mass percentage of clay fraction in bulk samples, the estimated total percentage of the smectitic layers were calculated. It varies from 0.10 % (STGA) to 1.94 % (CARO-G) and is well linked to spalling decay for CARO-G and VILL. Note that the low proportion of smectitic layers in BARB could be due to an incomplete < 4 µm separation.

4.3 Free swelling behavior

Free swelling experiments in both hydric and hygric conditions show that dilation can occur on reference stones aside from the presence of clay minerals (ESTA) but to a lower extent. On the stones strongly affected by spalling, maximum coefficients of hydric swelling are ranged from 0.46 (BIBE) to 1.75 $mm.m^{-1}$ (BARB) and are measured perpendicularly to the observed bedding plane Table 4.

SAMPLE	*MBA*	$\Delta l/l_{0\ hydric\ //}$	$\Delta l/l_{0\ hydric\ \perp}$	$\Delta l/l_{0\ hygric\ \perp}$	*Smectitic layers*		*Spalling decay*
	$mg.g^{-1}$	$mm.m^{-1}$	$mm.m^{-1}$	$mm.m^{-1}$	% < 4 µm	% sample	
BARB	9.5	0.61	1.75	0.112	31	0.29	++
BIBE	1.6	-	0.46	0.000	15	0.33	++
CARO-G	6.8	-	0.80	0.174	21	1.94	++
CARO-J	4.8	0.69	1.08	0.060	8	0.28	+
CRIL	9.2	0.34	0.57	0.029	17	0.18	+
ESTA	0.4	0.23	0.20	0.028	0	0.00	-
STGA	0.8	0.31	0.31	0.044	26	0.10	-
STSY	5.6	0.23	0.31	0.040	35	0.23	+
VILL	9.6	-	-	-	13	1.02	++

Table 4. Hydric and hygric dilation behavior of samples with corresponding values of MBA, smectitic layers proportions and observed spalling decay.

Dilation coefficients are ten times lower (from 0.000 to 0.174 $mm.m^{-1}$: Table 4) when measured in hygric conditions. The samples experiencing higher hydric dilatation have the highest hygric dilatation coefficients (BARB, CARO-G). It has to be point out that these sample correspond to those showing the higher degree of spalling *in situ*. However, BIBE limestone type presents both low hydric and hygric dilatation. This could be explained by the high radius medium measured that prevent water from access to reactive surfaces. The Figure 4 show the hygric dilation behavior through time of the reference samples (ESTA and STGA) in comparison to CARO-G and CARO-J.

Finally, results indicate that MBA values tend to be well correlated to the dilatation coefficients and could be used as a predicting test for the behavior of stones used in construction.

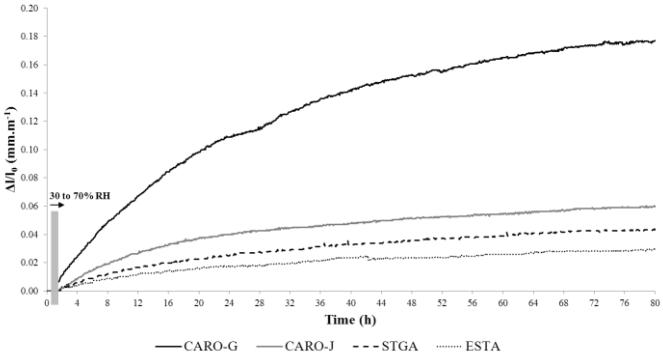

Figure 4. Hygric dilatation of limestones under relative humidity change from 30% to 70% and isothermal conditions through time.

5. Discussion

All the limestone types of "Pierre du Midi" studied experience dilation with respect to water saturation (hydric) or relative humidity increase (hygric). This observation leads to consider that swelling pressures are developed by the migration of water molecules in the porous media. Moreover, the correlation between the dilation coefficients and the degree of spalling decay *in situ* tends to confirm the mechanical impact of dimensional variations (Sebastian et al. 2008; Jimenez-Gonzalez et al. 2008). In addition, the measured dilation varies according to another factor: the clay content determined directly by gravimetric method or indirectly by the MBA test. Dimensional variations seem thus enhanced by the presence of clay minerals and more specifically smectitic layers. The proportions of these swelling clay minerals in glauconite/smectite mixed layer minerals are known to vary through the maturation process of glauconitic fillings (Meunier and El Albani 2007). This maturation process could thus be a natural factor of the heterogeneous behavior of the "Pierre du Midi" when used outdoor. As a significant example, the differences between the two facies of Caromb stone type can be explained by both the quantity of clay minerals and the smectitic proportions in the glauconite/smectite mixed layer minerals. These differences are translated macroscopically by greater dilation coefficients in CARO-G highlighting the triggering role of smectitic layers in dimensional variations.

As negatively charged particles, clay minerals are all subjected to osmotic swelling when a concentration gradient is provoked by the presence of an electrolyte (Sebastian et al. 2008). In addition, some clay minerals can experience intracristalline swelling caused by the hydration of the counter balancing cation of low charged layers (Moore and Reynolds 1997). In this case, the basal spacing is known to vary of about 70 % with the relative humidity or the water saturation (Colas et al. 2011; Wangler and Scherer 2008). With this phenomenon in mind, swelling clay minerals (such as smectites) are considered as precursors of dimensional variations of the "Pierre du Midi" as it has been

deducted elsewhere (Delgado-Rodrigues 2001; Franzini et al. 2007). At last, authors have reported that rock fabric, stress relaxation, elastic modulus and mechanical strength must be taken into account as limiting agent (Jimenez-Gonzalez et al. 2008) when explaining spalling decay. Thus further works will be done on the definition of the mechanicals parameters and on the behavioral answer of "Pierre du Midi" limestone types to relative humidity cycles variation.

Acknowledgements

This study was financially supported by the Provence Alpes Côtes d'Azur region, the Bureau de Recherches Géologiques et Minières (BRGM) and the Centre Interdisciplinaire de Conservation et de Restauration du Patrimoine (CICRP). The authors would like to thank Serge Nitsche and Damien Chaudanson (CINaM-CNRS) for their help and careful advices in electronic microscopy. The authors want also to tell their gratitude to Vincent Mercurio (CICRP) for sample preparation.

References

Benavente, D., Cultrone, G. and Gomez-Heras, M. 2008. 'The combined influence of mineralogical, hygric and thermal properties on the durability of porous building stones', *European Journal of Mineralogy*, **20**(1):673-685.

Colas, E., Mertz, J-D., Thomachot-Schneider, C., Barbin, V. and Rassineux, F. 2011. 'Influence of the clay coating properties on the dilation behavior of sandstones', *Applied Clay Science*, **52**(1-2):245-252.

Delgado-Rodrigues, J. 2001. 'Swelling behavior of stones and its interest in conservation. An appraisal', *Materiales de construccion*, **51**(263-264):183-195.

Dessandier, D., Blanc, A., Bromblet, P. and Mertz, J.D. 2002. 'Durabilité et compatibilité des pierres des monuments : proposition d'une méthodologie de sélection'. *Pierre Actual*, **791**(July):66-75.

Drits, V. A. and Tchoubar, C. 1991. 'X-ray diffraction by disordered lamellar structures: Theory and applications to micro divided silicates and carbons', *Crystal Research and Technology*, **26**(7):956.

Franzini, M., Leoni, L., Lezzerini, M. and Cardelli, R. 2007. 'Relationships between mineralogical composition, water absorption and hydric dilatation in the « Macigno » sandstones from Lunigiana (Massa, Tuscany)', *European Journal of Mineralogy*, **19**(1):113-123.

Jimenez-Gonzalez, I., Rodriguez-Navarro, C. and Scherer, G. W. 2008. 'Role of clay minerals in the physicomechanical deterioration of sandstone', *Journal of Geophysical Research*, **113**(F2): F02021.

Meunier, A. 2002. *Argiles*, Paris: GB Sciences Publisher.

Meunier, A. and El Albani, A. 2007. 'The glauconite-Fe-illite-Fe-smectite problem: a critical review', *Terra Nova*, **19**(2):95-104.

Moore, D. M. and Reynolds, R. C. Jr. 1997. *X-ray Diffraction and the Identification and Analysis of Clay Minerals.* New York: Oxford University Press.

Sebastian, E., Cultrone, G., Benavente, D., Fernandez, L. L., Elert, K. and Rodriguez-Navarro, C. 2008. 'Swelling damage in clay-rich sandstones used in the church of San Mateo in Tarifa (Spain)', *Journal of Cultural Heritage*, **9**(2):66-76.

Vergès-Belmin V., 2008. 'Illustrated glossary on stone deterioration patterns a Glossaire illustré sur les forms d'altération de la pierre', *Monuments & Sites 15*. Paris: ICOMOS and ISCS.

Wangler, T. and Scherer, G. W. 2008. 'Clay swelling mechanism in clay-bearing sandstones'. *Environmental Geology*, **56**(3-4):529-534.